Residual energy and its effect on gain in a Lyman-α laser

P. Pulsifer, J. P. Apruzese, J. Davis, and P. Kepple
Radiation Hydrodynamics Branch, Plasma Physics Division, Naval Research Laboratory, Washington, D.C. 20375-5346
(Received 22 September 1993)

To examine prospects for gain in a Lyman-α recombination laser driven by a high-intensity, short-pulse laser, we calculate the residual energy in both hydrogen and helium during recombination after the ionizing pulse. The expected gain as a function of residual energy and density is then separately evaluated. The residual energy calculation includes above-threshold ionization (ATI) in the presence of a background plasma, as well as inverse-bremsstrahlung heating. At electron densities over 10^{18} cm^{-3} but below critical density, the plasma reduces the ATI energy by approximately a factor of 2, but without a previously reported dependence on the pulse width. Inverse-bremsstrahlung heating can be significant, but is not dominant for the parameters considered. Detailed recombination-laser gain calculations were performed for the Ly-α transitions of both H and He, using Stark profiles to represent the laser line cross section. To obtain gain of near 2 cm^{-1} lasting at least a few ps, the H plasma temperature must be less than 3.5 eV and electron density between 4×10^{17} and 4×10^{18} cm^{-3}; for He, the temperature must be less than 15 eV and the electron density between 2×10^{18} and 2×10^{19} cm^{-3}. Our calculations indicate that these conditions can be satisfied for H, if the driving laser intensity is above 4×10^{14} W cm^{-2}, and for He, if the laser intensity is above 1.7×10^{16} W cm^{-2} and the wavelength is below 0.6 μm.

PACS number(s): 42.55.Vc, 32.80.Rm, 52.40.Nk, 52.50.Jm

I. INTRODUCTION

The possibility of developing a recombination x-ray laser that is driven by the new short-pulse, high-intensity table-top lasers has recently been considered [1–5]. With sufficiently high intensity, a population inversion can be obtained with large transition energies (such as those involving the ground state), which can generate significant gain at UV or soft x-ray wavelengths. These schemes require both that the atoms initially be ionized above the lasing stage and that the residual energy of the electrons be low to facilitate recombination and suppress collisional excitation.

In this paper, we analyze the conditions required for gain on the Lyman-α transitions of both hydrogen (1216 Å) and helium (304 Å). Such lasers were initially proposed some years ago [6]. Our gain calculations are based on fully self-consistent Stark profiles for the completely stripped background gas. The residual energy is calculated including the electron above-threshold-ionization (ATI) energy, a simple model of plasma effects, and inverse-bremsstrahlung, or collisional, heating.

To obtain the ATI energy, we follow a well-established procedure [1,7] and solve for the classical (nonrelativistic, nonquantum) electron motion; the ATI energy is just the electron's energy long after the pulse has passed (after several ps, when recombination is occurring).

Particle-in-cell (PIC) simulations [8] have indicated that space charge, or plasma effects, might in some way significantly enhance or diminish the energy absorption of the target medium. For short pulse lengths, comparable to the inverse plasma frequency, space-charge heating apparently stems from the nonadiabatic ponderomotive expulsion of electrons (electron cavitation), which induces plasma oscillations. An early study [8] sought to model plasma effects on ATI energy by including the plasma frequency in the single-electron equation of motion; it found that the plasma-modified ATI energy was fairly large, but oscillated by several orders of magnitude as a function of electron density and pulse period. Here, we use the same model, but our findings disagree with those results: the ATI energy is much lower, and there are no oscillations with electron density. For this simple model, the principal effect of a background plasma is to substantially increase the residual energy near the critical surface. These results are more in accord with those of other recent theoretical and experimental papers [9,10], are not inconsistent with the PIC simulations in Ref. [8], and are in fact more favorable to the success of a Ly-α laser.

One potentially important factor that has not been widely considered is inverse-bremsstrahlung heating [9]. Simple scaling arguments indicate that this could be a much larger source of energy to the plasma than the ATI mechanism. In fact, for the parameters we consider, inverse bremsstrahlung does not turn out to be the most important source of heating, largely because the high quiver energy of the electrons in the field makes the electron-ion collisional cross section small during the bulk of the heating.

The organization of this paper is as follows. In Sec. II, we consider ionization and electron heating by the laser pulse, and show how to obtain the residual energy during recombination. In Sec. III, we consider the recombination process, and show what conditions must be satisfied by the plasma to obtain significant gain. These results will show the optimal pump laser parameters for driving the recombination laser. Possible experimental parameters are discussed in the final section.

II. CALCULATION OF ELECTRON RESIDUAL ENERGY

We consider a laser pulse of wavelength λ (in μm) and peak intensity I (in W cm^{-2}), incident onto an initially neutral gas, which has atomic charge Ze. (An electron has charge $-e$ and mass m.) The laser pulse profile is assumed to be such that the electric field is given by $E(t)=E_{\rm env}(t)\sin\omega t$, with the pulse envelope given by

$$E_{\rm env}(t)=E_0\,\mathrm{sech}\left[\frac{2(t-t_{\rm max})}{\tau_p}\right] \tag{1}$$

and the peak electric field $E_0=(240\pi I)^{1/2}$ (in V/cm). For the calculations presented here, we consider a pulse width $\tau_p=100$ fs and time of maximum intensity $t_{\rm max}=200$ fs. The intense laser field multiply ionizes the gas, and the ion densities n_i (in cm^{-3}) for charge state $Z_i=i$ evolve according to the coupled system of equations

$$\frac{dn_i}{dt}=W_i n_{i-1}-W_{i+1}n_i\ , \tag{2}$$

where W_i is the rate of ionization from charge state Z_{i-1} to Z_i, and $n_{-1}=W_{Z+1}\equiv 0$. The evolving electron density is $n_e=\sum_i Z_i n_i$. We assume that the laser pulse duration is much shorter than the recombination time, so that during the pulse recombination can be neglected.

There are various theories of ionization in the strong-field regime [7]. For ATI conditions, considered here, the photon energy ($\hbar\omega=1.24/\lambda$ eV) is less than the ionization energy U_i, which in turn is less than or equal to the electron quiver energy (defined below). Here, tunneling ionization might be expected to dominate, and the ionization rate can be obtained from either Keldysh [11] or Ammosov, Delone, and Kraĭnov [12]. For the calculations presented here, we use the Ammosov formula [12], which has some experimental support [13], and is also considerably simpler to evaluate. The Ammosov rate is

$$W_i(E)=1.61\omega_{\rm a.u.}\frac{Z_i^2}{n_i^{*4.5}}\left[10.87\frac{Z^3}{n_i^{*4}}\frac{E_{\rm a.u.}}{E}\right]^{2n_i^*-1.5}\times\exp\left[-\frac{2Z_i^3}{3n_i^{*3}}\frac{E_{\rm a.u.}}{E}\right]\ , \tag{3}$$

where the atomic unit of frequency $\omega_{\rm a.u.}=4.1340\times10^{16}$ sec^{-1}, n_i^* is the effective principal quantum number for a hydrogenic atom:

$$n_i^*=\frac{Z_i}{\sqrt{U_i/13.6\ \mathrm{eV}}}\ , \tag{4}$$

and $E_{\rm a.u.}=5.1421\times10^9$ V/cm is the electric field at a ground-state hydrogen electron.

At the time of ionization, we assume that electrons have zero energy [1]; thereafter, they are (classically) accelerated by fields from the laser and from the surrounding plasma [8]. Most of the electron energy during the laser pulse comes from the oscillatory quiver motion in the laser field, and is returned to the field when the pulse passes. The relatively small residual energy after the pulse leaves is the ATI energy. When the effect of the plasma is ignored, the ATI energy is the time-independent part of the energy, which is determined by the wave phase at ionization. With a plasma oscillation present, there is no time-independent part of the energy, so the ATI energy must be an average energy. To find it, we follow the classical trajectory $x(t)$ of an electron, with the effect of the charge cloud of the surrounding plasma being treated solely as a springlike restraining force [8] parametrized by the plasma frequency $\omega_p=(4\pi n_e e^2/m)^{1/2}$,

$$\ddot{x}+\omega_p^2 x=-\frac{e}{m}E(t)\ . \tag{5}$$

The required boundary condition on Eq. (5) is that $\dot{x}=0$ at the ionization time $t=t_0$. With the additional imposed condition that $x(t_0)=0$, the general solution to Eq. (5) can be expressed as

$$x(t)=-\frac{\cos\omega_p t}{\omega_p}\int_{t_0}^{t}\frac{eE(t)}{m}\sin\omega_p t\,dt+\frac{\sin\omega_p t}{\omega_p}\int_{t_0}^{t}\frac{eE(t)}{m}\cos\omega_p t\,dt\ . \tag{6}$$

If the electric-field envelope were constant, as it roughly is near the peak of the pulse, the solution would be similar to that obtained elsewhere [8],

$$x(t)=\frac{eE_{\rm env}}{m(\omega^2-\omega_p^2)}\{-\sin\omega t+[\omega\cos\omega t_0\cos\omega_p t_0+\omega_p\sin\omega t_0\sin\omega_p t_0]\sin\omega_p t+[-\omega\cos\omega t_0\sin\omega_p t_0+\omega_p\sin\omega t_0\cos\omega_p t_0]\cos\omega_p t\}\ . \tag{7}$$

This describes the complicated electron motion during the pulse, but is not really useful for finding the ATI energy, which is determined much later. The electron motion at those late times, obtained from the $t\to\infty$ limit of Eq. (6), is just simple oscillation at the plasma frequency,

$$\dot{x}(t_0,t)=\frac{eE_0}{m}[A\sin\omega_p t+B\cos\omega_p t] \tag{8}$$

with

$$A(t_0)\equiv\int_{t_0}^{\infty}\mathrm{sech}\left[\frac{2(t-t_{\rm max})}{\tau_p}\right]\sin\omega t\sin\omega_p t\,dt\ , \tag{9}$$

$$B(t_0)\equiv\int_{t_0}^{\infty}\mathrm{sech}\left[\frac{2(t-t_{\rm max})}{\tau_p}\right]\sin\omega t\cos\omega_p t\,dt\ . \tag{10}$$

The time dependence of the factors A and B can be ignored because the laser pulse (sech) vanishes for late time; they depend only on the time t_0 when the electrons are ionized. If the plasma period is smaller than the times of interest (the ns recombination time), the single-electron ATI energy is the electron energy averaged over the plasma-frequency motion,

$$\epsilon(t_0)\equiv\tfrac{1}{2}m\langle\dot{x}^2\rangle=\epsilon_q\omega^2(A^2+B^2)\ , \tag{11}$$

where

$$\epsilon_q\equiv\frac{e^2E_0^2}{4m\omega^2} \tag{12}$$

is the quiver, or ponderomotive, energy.

The average electron residual energy $\langle\epsilon\rangle$ after the passage of the pulse is given by the sum of the number of electrons generated at each t_0 times the residual energy of these electrons,

$$\langle\epsilon\rangle=\frac{\sum_{j=1}^{z_{\max}}\int_0^{2t_{\max}}n_j(t_0)W_j(E(t_0))\epsilon(t_0)dt_0}{\sum_{j=1}^{z_{\max}}\int_0^{2t_{\max}}n_j(t_0)W_j(E(t_0))dt_0}\ . \tag{13}$$

The upper limit of integration is chosen as $2t_{\max}$ here simply for convenience, to make the integration domain symmetrical over the pulse; the results should not be sensitive to the value chosen for this limit, as long as the pulse amplitude is small there. For simplicity, the influence of the space-charge field on the ionization rate $W(E)$ has been neglected, although PIC simulations [8] have indicated that electron cavitation, when significant, can produce a space-charge electric field comparable to the laser field $E(t)$. The simple model used here could be extended in that case by deducing the space-charge field at the points of interest (subject to details of pulse profile and ionization dynamics) and then using the total field in Eq. (13). We define the residual electron temperature to be proportional to the average energy,

$$T=\tfrac{2}{3}\langle\epsilon\rangle\ . \tag{14}$$

When the laser pulse width is very broad compared to the oscillator frequency and plasma frequency (i.e., $\omega\tau_p\gg1$ and $\omega_p\tau_p\gg1$), then the integrals of A and B can be approximately evaluated, and

$$\epsilon(t_0)\approx\frac{e^2E(t_0)^2}{4m}\left[\frac{\omega_p^2\sin^2\omega t_0+\omega^2\cos^2\omega t_0}{(\omega^2-\omega_p^2)^2}\right]\ . \tag{15}$$

This expression shows that, long after the pulse, plasma effects do not decrease the residual energy. There is no periodic dependence on the plasma frequency in the residual energy, as was asserted elsewhere [8]. That periodic variation was based on an ATI energy calculated from some average of Eq. (7), and so incorrectly included electron motion during the pulse in the ATI energy calculation. In fact, plasma effects can increase the residual energy, but the effect is not important except near the critical surface, where the plasma and wave frequencies are near resonance and the residual energy becomes very large.

When the density is zero (no plasma) the single-particle ATI energy from Eq. (15) is

$$\epsilon(t_0)=\epsilon_q\cos^2\omega t_0\ , \tag{16}$$

which is half the standard zero-density result [1]. The factor-of-2 difference is due to the averaging over a plasma period performed in Eq. (15); this averaging makes sense only when the plasma frequency is large, while for low densities the peak value of the electron energy should be used. The density effect on residual energy depends on the ratio $\omega_p^2/\omega^2=n_e/n_{\rm crit}$, where $n_{\rm crit}=1.12\times10^{21}/\lambda^2$ is the critical density, where the plasma becomes opaque to the laser radiation. The single-particle ATI energy from Eq. (15) is shown in Fig. 1, where separate curves are drawn for different ionization phases ωt_0. As the density approaches $n_{\rm crit}$, the ATI energy sharply increases, and becomes less dependent on the time of ionization t_0.

Evidently, plasma does not significantly increase the ATI energy at much less than $0.1n_{\rm crit}$. For 1.06-μm Nd:glass laser light, the $n_{\rm crit}=10^{21}$ cm^{-3}, while for a 248-nm KrF laser $n_{\rm crit}=2\times10^{22}$ cm^{-3}; thus, according to our simple model, plasma modification of the ATI energy is not a significant factor below densities of 10^{20} cm^{-3}.

Collisional heating from inverse bremsstrahlung is potentially important, possibly dominant, in dense laser-heated plasmas [9]. The inverse-bremsstrahlung heating rate is given by

$$\dot{E}_{\rm IB}=\frac{4\pi}{3}\epsilon_q\nu_{ei}v_{\rm th}^3f_0(0)F(v_0/v_{\rm th})\ , \tag{17}$$

where $f_0(v)$ is the isotropic part of the electron distribution function, $v_{\rm th}=(2kT/m)^{1/2}$ is the thermal velocity (with kT the electron temperature in energy units),

$$\nu_{ei}=3.86\times10^{-6}\frac{Zn_e}{(kT)^{3/2}}\ln\Lambda \tag{18}$$

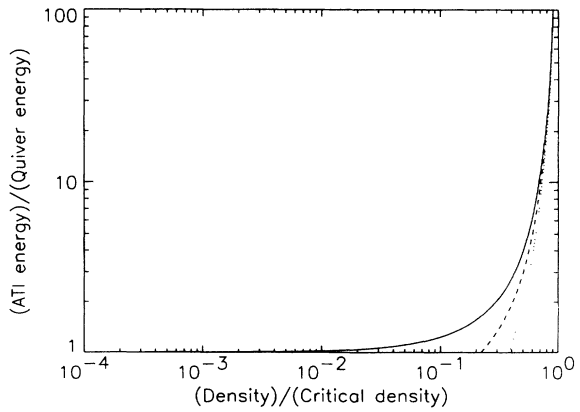

FIG. 1. Effect of the plasma oscillation on the single-particle ATI energy. The ATI energy, in units of the quiver energy ϵ_q, is shown as a function of density, in units of the critical density $n_{\rm crit}$, for different times of ionization within the pulse ωt_0. The solid line is for $\omega t_0=0$, when the zero-density ATI energy is maximum; the dashed line is for $\omega t_0=\pi/4$; and the dotted line is for $\omega t_0=\pi/2$, when the zero-density ATI energy is zero.

is the electron-ion collision frequency, with Coulomb logarithm given by

$$\ln\Lambda = 22.4 + \ln[(kT)^{3/2}/n^{1/2}] , \tag{19}$$

and F is a correction factor to the cross section due to the quiver motion of the electrons [14], which may be approximated

$$F(x) = \frac{1}{1+2x^2/3} . \tag{20}$$

The rate $\dot{E}_{IB}$ depends on the electron distribution only through the overall normalization, and is not sensitive to the details of its shape. Therefore, although the laser-produced electrons equilibrate on the ps to tens of ps time scale (much longer than the pulse width), it is not too inaccurate to approximate the distribution function to be a Maxwellian, so that

$$f_0(0) = n_e \left[\frac{m}{2\pi kT}\right]^{3/2} . \tag{21}$$

To estimate the magnitude of inverse-bremsstrahlung heating, we determine the total energy input by time-integrating the heating rate, Eq. (17). The heating rate depends on the time-varying electron density, obtained by solving the rate equations, Eq. (2). The temperature at each time is given by the average energy per particle, as accumulated from ATI (a small term), prior inverse-bremsstrahlung heating, and the quiver motion (a large term). The inverse-bremsstrahlung contribution to the final temperature is just the total average energy input per particle,

$$T_{IB} = \frac{2}{3n_e}\int_0^\infty \langle \dot{E}_{IB} \rangle dt . \tag{22}$$

The actual residual temperature is given by the sum of contributions from ATI [Eq. (14)] and IB heating [Eq. (22)]. Results of residual energy calculations are shown in Figs. 2–5. The contours in Fig. 2 depict the average degree of ionization after the laser pulse of an initially neutral H gas, as a function of laser intensity and wavelength; any laser power above the $\bar{Z}=1$ contour leaves

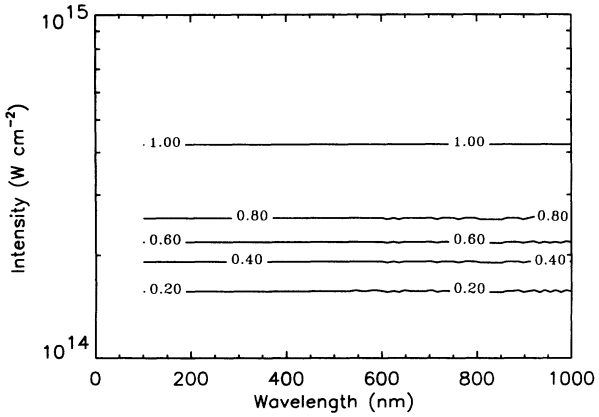

FIG. 2. Residual ionization contours for initially neutral H. Contours represent average ionization level $\bar{Z}=n_e/n_H$; for laser intensity above the $\bar{Z}=1$ contour, the gas is left fully stripped.

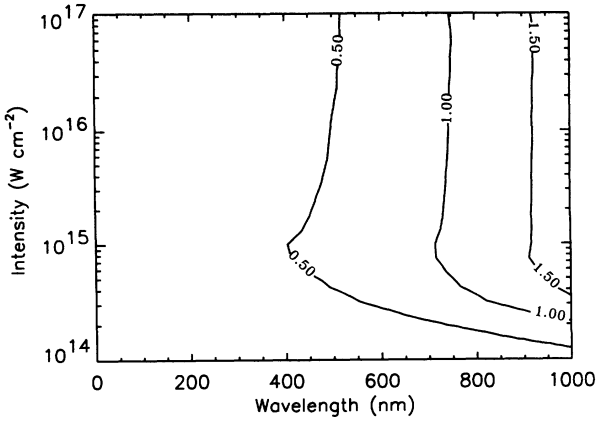

FIG. 3. Contours of residual temperature in eV of H, as described in Fig. 2. For inverse-bremsstrahlung heating calculations, an initial atomic density of 2×10^{18} cm^{-3} is assumed.

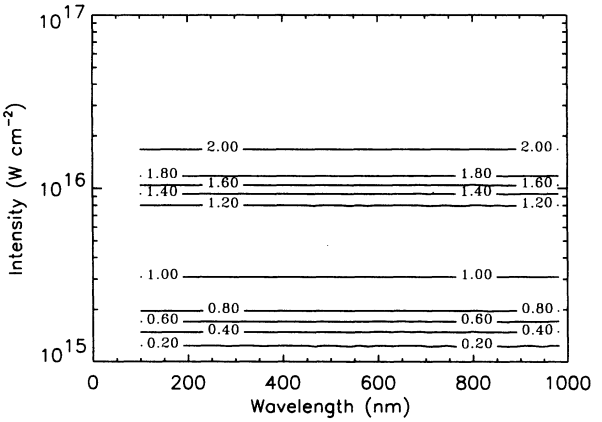

FIG. 4. Residual ionization contours for initially neutral He. Contours represent average ionization level $\bar{Z}=n_e/n_{He}$; for laser intensity above the $\bar{Z}=2$ contour, the gas is left fully stripped.

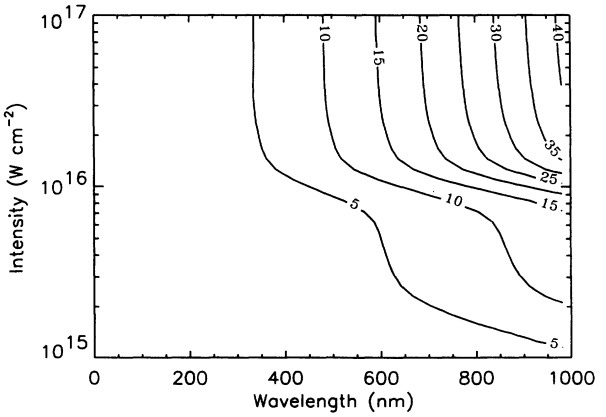

FIG. 5. Contours of residual temperature in eV of He, as described in Fig. 4. For inverse-bremsstrahlung heating calculations, an initial atomic density of 4×10^{18} cm^{-3} is assumed.

the gas fully stripped. The contours in Fig. 3 show the residual temperature in eV of the ionized H plasma. The inverse-bremsstrahlung heating rate is proportional to n_e; here, an atomic density of 2×10^{18} cm^{-3} was used, where there is relatively high gain. Similarly, Fig. 4 depicts the average degree of ionization after the laser pulse of an initially neutral He gas, and Fig. 5 shows the residual temperature in eV as a function of laser wavelength and intensity. For He, the inverse-bremsstrahlung heating rate was computed using an atomic density of 4×10^{18} cm^{-3}.

III. CONDITIONS REQUIRED FOR GAIN ON Ly-α FOR HYDROGEN AND HELIUM

It is reasonable to assume that gain on Ly-α via transient recombination [6] would be easiest to achieve in the lowest atomic number elements. Therefore, we examine H and He closely using time-dependent multilevel gain calculations to establish the electron temperature (i.e., residual energies) and densities at which reasonable amplification would occur. These can be related to the short-pulse laser parameters which are predicted to provide such conditions according to the calculations of Sec. II. In this way, we specify what would constitute a promising demonstration experiment.

The first and well known condition for transient gain to the ground state is that the plasma be initially fully stripped [6]. Therefore, laser irradiances must be used that are at or above those in the contour plots (Figs. 2–5) corresponding to $Z=1$ for H and $Z=2$ for He. In all the calculations discussed below, the plasma is assumed initially fully stripped. The atomic-level populations are calculated as a function of time for a fixed assumed density and electron temperature. The ions are assumed to remain cold, since their equilibration time (a few hundred ps) at the densities of interest far exceeds the time scales within which gain is expected. The algorithm of Ref. [15] is employed to integrate the set of rate equations, viz.,

$$\frac{dN_i}{dt}=\sum_{j\neq i}N_jR_{ji}-N_i\sum_{j\neq i}R_{ij}\ , \tag{23}$$

where N_i is the population density of the state i and R_{ji} are the rates connecting all states; these atomic-level rates and densities are not to be confused with the ionization-state rates and densities of Eq. (2).

In Eq. (23), the rates connecting the various levels of the H and He states include collisional excitation and deexcitation, radiative, three-body, and dielectronic recombination, collisional ionization, and radiative decay. Most of the atomic data for these simple and well-studied species are readily available from numerous sources in the literature. Other rates were calculated using standard techniques (e.g., the semiclassical approximation for collisional rates corresponding to radiatively allowed collisions). The levels of the one-electron species are distinguished only by principal quantum number n, although fine structure effects on Ly-α are included in the overall Stark profile used in calculating gain.

The highest principal quantum number included in the atomic model is $n=5$ for both H and He. This is approximately in accord with the Inglis-Teller criterion as updated by Griem (Ref. [16], p. 125). At an electron density of 10^{18} cm^{-3}, Ref. [16] predicts that the series limit occurs at $n=4$–5 for H, and $n=6$–7 for He. While we do not include a self-consistent treatment of continuum lowering, it is clearly preferable to truncate the levels at $n=5$ rather than at some arbitrary higher number (10 or 20, for instance), far above the last discrete level at densities of interest.

The gain g in cm^{-1} on the $n=2$ to 1 transition of a hydrogenic species is given by

$$g=N_2\sigma_{21}-N_1\sigma_{12}\ , \tag{24}$$

where σ_{21} (σ_{12}) are the emission (absorption) cross sections in cm^2 for the transition at the peak of the profile and the N's are the population densities of the $n=1$ and 2 levels. In Eq. (24) a positive number corresponds to amplification and a negative one to absorption. For Ly-α, $\sigma_{21}=\sigma_{12}/4$, and $n=2$ must have at least 4 times the population of the ground state to obtain gain. Clearly, this can only occur on a transient basis since population tends to pile up in $n=1$, which has no radiative decay channel. However, three-body recombination from the bare nucleus, per unit statistical weight, is approximately proportional to n^4/T. Therefore, one anticipates a brief period of gain for an appropriate range of sufficiently low temperatures, if $n=1$ is initially empty.

A key feature of the present work is that we have employed the best available representation of the Ly-α cross section, namely self-consistently calculated Stark profiles for both H and He [17]. For H, we find that σ_{12} is approximately given by

$$\sigma_{12}^{\mathrm{H}}=6.1\times10^{-15}\left[\frac{10^{18}}{n_e}\right]^{0.89}T^{0.25}\ , \tag{25a}$$

whereas, for He,

$$\sigma_{12}^{\mathrm{He}}=2.5\times10^{-14}\left[\frac{10^{18}}{n_e}\right]^{0.93}\left[\frac{T}{5}\right]^{0.25}\ . \tag{25b}$$

For $T\propto Z^2$, the He cross section exceeds that of H by a factor of 4 at $n_e=10^{18}$ cm^{-3}. Partly offsetting this, however, is the fact that there are twice as many H ions per electron as He ions. Therefore, we expect gains of comparable magnitude. Also, note from Eq. (25) that as the density increases, the Stark broadening results in a nearly inversely proportional decrease of the peak cross section. However, gain can still increase with density due to the increase in three-body recombination and the greater number of ions available for stimulated emission.

A subset of the calculations that have been carried out for H and He is presented in Figs. 6–10. There is no lower temperature limit below which gain is not possible; indeed, due to the T^{-1} dependence of three-body recombination, gain increases at lower temperatures, assuming, of course, that the plasma is initially fully stripped. To obtain a gain of ~2 cm^{-1} lasting at least a few ps, the electron temperature in a He plasma must be ≤15 eV, whereas for H the electrons must be no hotter than 3.5 eV. An upper limit on the density is set by the desired gain duration. Note from Figs. 6–10 that, as expected,

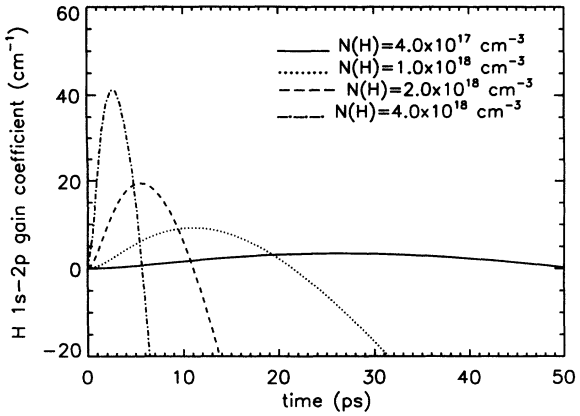

FIG. 6. Ly-α gain coefficient for H as a function of time, assuming an initially fully stripped plasma of the indicated atomic densities. Electron temperature is 1 eV; ions are assumed cold and Stark profiles are employed to obtain the gain cross section.

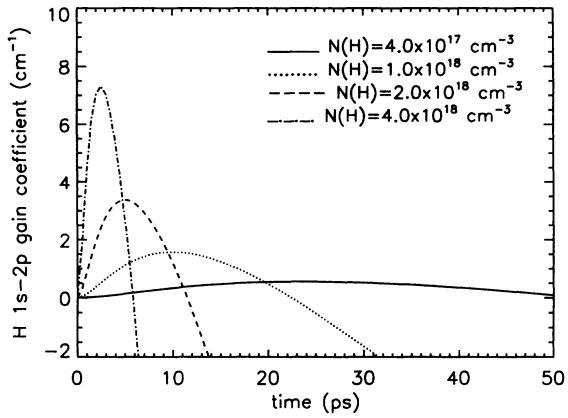

FIG. 7. As in Fig. 6 except that the electron temperature is 2 eV.

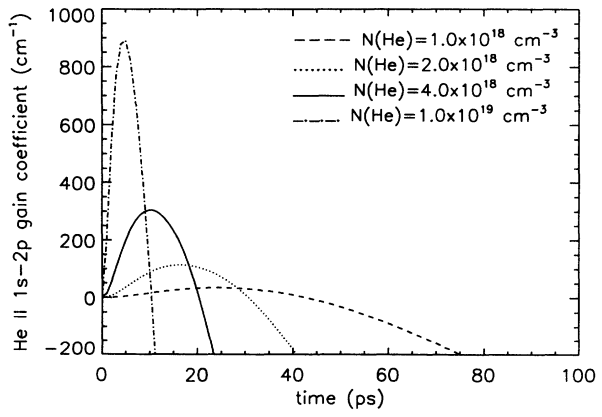

FIG. 8. Ly-α gain coefficient for He as a function of time, assuming an initially fully stripped plasma of the indicated atomic densities. Electron temperature is 2 eV; ions are assumed cold and Stark profiles are employed to obtain the gain cross section.

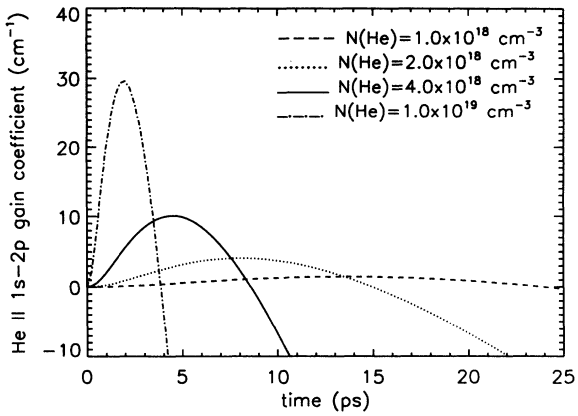

FIG. 9. As in Fig. 8 except that the electron temperature is 5 eV.

the gain increases with density, but decreases with increasing temperature. However, the duration of gain decreases sharply with increased density since the absorbing $n=1$ level fills up correspondingly more rapidly. For gain duration of at least a few ps, the electron density must be no higher than $\sim 2\times 10^{19}$ cm^{-3} for He, or 4×10^{18} cm^{-3} for H. Since the lifetime of the H Ly-α transition (n averaged) is 2.1 ns, compared to 133 ps for He, one might initially expect considerably greater gain duration for H. However, the corresponding collisional mixing rates are nearly an order of magnitude faster for H at a given density, and the interplay of these effects results in comparable gain durations for both elements (ranging from a few ps to tens of ps).

Refraction of the x-ray laser beam can pose a serious threat to the practical attainment of amplification, due to the density gradients expected in short-pulse laser-driven plasmas. This issue has been analyzed by Amendt *et al.* [5], who assumed a Gaussian beam profile. If b is the beam waist radius, the x-ray lasing length Z_R is approximately given by

$$Z_R = 1.2b\left[\frac{n_{\rm crit}}{n_e}\right]^{1/2}, \tag{26}$$

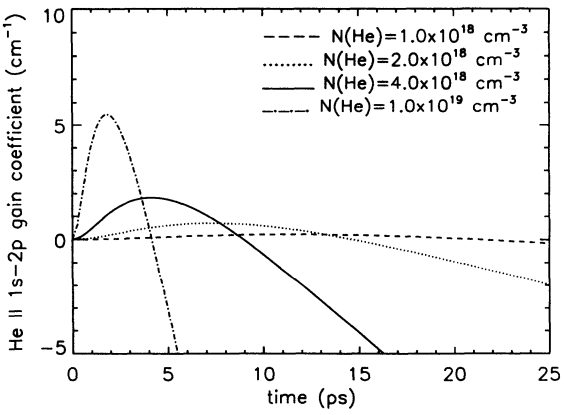

FIG. 10. As in Figs. 8 and 9, except that the electron temperature is 10 eV.

where n_{crit} is the critical density, defined above. Typical electron densities for good gain in H and He are 2 and 4×10^{18} cm^{-3}, respectively (cf. Figs. 6–10). We take the beam waist radius to be 13 μm, as measured in a recent demonstration of optical guiding of intense laser beam pulses [18]. For these conditions, Eq. (26) gives a propagation length of 0.3 cm for H and 0.9 cm for the considerably shorter wavelength of the He laser. Figures 8 and 9 indicate that gain-length products (gl) greater than or equal to 4 are achievable for He if $T_e \leq 5$ eV. For H, $T_e \leq 1$ eV is necessary to achieve a similar gl. As pointed out in Ref. [5], a larger beam waist radius would significantly relax these requirements. In addition, the presence of a beam guiding channel [18] with a more favorable refractive index profile would very likely lead to considerably longer propagation lengths.

IV. SUMMARY AND CONCLUSIONS

We have presented a procedure to calculate the residual energy of a plasma during the recombination period after passage of a high-intensity, short laser pulse. We then calculated the expected residual energy and degree of ionization for H and He over a range of wavelengths and laser intensities. These results are shown as contour plots in Figs. 2–5. The inclusion of a plasma oscillation does not significantly modify the residual electron energy [other than the factor-of-2 reduction due to the residual plasma oscillation, as discussed at Eq. (16)], as long as the plasma density is not close to the critical density.

While our model does not include it, we do not expect the space-charge heating reported in PIC simulations [8,10] to be important for parameters where significant gain should be found. The short pulse width limits heating due to instability growth and variations in drift velocities [10]. The laser power required is not ultrahigh (i.e., $I \ll 10^{18}$ W cm^{-2}), and the density is relatively high, so both electron cavitation and its effect on the final plasma temperature [8] should be minimal; even if this were not true, electron-cavitation heating seems to be much less important when $\omega_p \tau_p / 2\pi > 1$, which is the case for the high-gain densities given here.

Although certainly not conclusive, it is gratifying to note that our results are close to recent experimental measurements by Mohideen *et al.* [19]. Their experiment measured residual energy in a low-density (7×10^8 atoms cm^{-3}) He gas, where the factor of $\frac{1}{2}$ from averaging over the late-time plasma oscillation in Eq. (16) should be omitted. The laser wavelength was 0.820 μm, with intensity 7×10^{15} W cm^{-2} and pulsewidth 180 fs. Although their pulsewidth was slightly longer than assumed here (which would tend to increase the residual energy), Fig. 5 shows that for these parameters the predicted residual temperature is roughly 20 eV, compared to the 30 eV measured best-fit temperature.

Through the residual energy and ionization calculations, we have established the plasma conditions during recombination. We have then used an inclusive atomic model to calculate gain and those conditions for which significant gain is obtained. These results are shown in Figs. 6–10. The region in the contour plots where the plasma is both fully stripped and has residual energy within the given limits is where gain is expected. For H, fully stripped plasma is obtained at intensities above 4×10^{14} W cm^{-2}; the necessary electron temperature, less than 3.5 eV, is satisfied at all wavelengths. For He, fully stripped plasma is obtained when the laser intensity is above 1.7×10^{16} W cm^{-2}; if this is true, the electron temperature is below the maximum 15 eV when the wavelength is below 0.6 μm.

The minimum density for which adequate gain is obtained can be seen from Figs. 6–10 to be roughly 10^{18} cm^{-3}. Although the residual energy increases with increased density, mostly because of inverse-bremsstrahlung, the most important effect is the decrease in gain duration (for a fixed residual energy) with increased density; this limits the electron density to roughly 4×10^{18} cm^{-3} for H, or 2×10^{19} cm^{-3} for He.

The simple model used here notably omits consideration of collisions. At typical laser-heated plasma parameters of $kT=10$ eV and $n=2\times10^{18}$ cm^{-3}, the collision time is about 0.8 ps. Thus, these plasmas are marginally collisional, and collision effects should be studied. Still, collisions do not clearly dominate, and there is probably some validity, at least for simple estimates, to the residual electron energies given here.

ACKNOWLEDGMENTS

This work was supported jointly by BMDO/T/IS and ONR.

[1] N. H. Burnett and P. B. Corkum, J. Opt. Soc. Am. B **6**, 1195 (1989).
[2] P. Amendt, D. C. Eder, and S. C. Wilks, Phys. Rev. Lett. **66**, 2589 (1991).
[3] D. C. Eder, P. Amendt, and S. C. Wilks, Phys. Rev. A **45**, 6761 (1992).
[4] P. Amendt, D. C. Eder, R. A. London, and M. D. Rosen, Phys. Rev. A **47**, 1572 (1993).
[5] P. Amendt, D. C. Eder, R. A. London, B. M. Penetrante, and M. D. Rosen, in *Short-Pulse High-Intensity Lasers and Applications,* edited by H. A. Baldis, SPIE Conf. Proc. No. 1860 (SPIE, Bellingham, WA, 1993), p. 140.
[6] W. W. Jones and A. W. Ali, Appl. Phys. Lett. **26**, 450 (1975); J. Appl. Phys. **48**, 3118 (1977).
[7] R. R. Freeman and P. H. Bucksbaum, J. Phys. B **24**, 325 (1991).
[8] B. M. Penetrante and J. N. Bardsley, Phys. Rev. A **43**, 3100 (1991).
[9] S. C. Rae and K. Burnett, Phys. Rev. A **46**, 2077 (1992).
[10] W. P. Leemans, C. E. Clayton, W. B. Mori, K. A. Marsh, P. K. Kaw, A. Dyson, C. Joshi, and J. M. Wallace, Phys. Rev. A **46**, 1091 (1992).
[11] L. V. Keldysh, Sov. Phys. JETP **20**, 1307 (1965).
[12] M. V. Ammosov, N. B. Delone, and V. P. Kraĭnov, Sov. Phys. JETP **6**, 1191 (1986).
[13] S. Augst, D. Strickland, D. D. Meyerhofer, S. L. Chin,

and J. H. Eberly, Phys. Rev. Lett. **63**, 2212 (1989).
[14] L. Schlessinger and J. Wright, Phys. Rev. A **20**, 1934 (1979).
[15] T. R. Young and J. P. Boris, J. Phys. Chem. **81**, 2424 (1977).
[16] H. R. Griem, *Plasma Spectroscopy* (McGraw-Hill, New York, 1964).
[17] P. C. Kepple, Phys. Rev. A **6**, 1 (1972).
[18] C. G. Durfee III and H. M. Milchberg, Phys. Rev. Lett. **71**, 2409 (1993).
[19] U. Mohideen, M. H. Sher, H. W. K. Tom, G. B. Aumiller, O. R. Wood III, R. R. Freeman, J. Bokor, and P. H. Bucksbaum, Phys. Rev. Lett. **71**, 509 (1993).